18. cAMP production was measured in cells that were shaken in phosphate buffer for 4 hours, followed by 50-nM pulses of cAMP for an additional 3 hours (*28*). Cells were then collected, washed twice, and resuspended at 5×10^7 cells/ml. They were then stimulated with 10 μM 2′-deoxy-cAMP, dithiothreitol was added to a final concentration of 5 mM, and 100-μl samples were removed at various times, added to 100 μl of 3.5% perchloric acid, and frozen. Total cAMP produced was determined with a cAMP RIA kit (Amersham). Before analysis, frozen samples were thawed and neutralized with 50% $NaHCO_3$, the resulting lysates were centrifuged, and the supernatants were assayed. Total cAMP production of cells developing on filters was determined by scraping cells directly into 3.5% perchloric acid and processing the samples as described above. The cAMP standard curves were determined by processing known concentrations of cAMP through the same sample preparation as the stimulated cells (perchloric acid treatment and so forth). Sensitivity to beef heart phosphodiesterase (Sigma) was used to confirm the presence of cAMP in samples. PDE treatment lowered cAMP concentrations in wild-type samples to those measured in *acaA* mutant strains. The amounts of "cAMP" measured in extracts of *acaA*-null or *acaA*(PKA-C) cells were unaffected by the treatment with PDE. In these experiments, the detection limit of the assay was 0.1 pmol per 10^7 cells.
19. W. Roos, C. Scheidegger, G. Gerisch, *Nature* **266**, 259 (1977); K. J. Tomchik and P. N. Devreotes, *Science* **212**, 443 (1981); H. Levine, I. Aranson, L. Tsimring, T. V. Truong, *Proc. Natl. Acad. Sci. U.S.A.* **93**, 6382 (1996).
20. E. Wallraff, D. L. Welker, K. L. Williams, G. Gerisch, *J. Gen. Microbiol.* **130**, 2103 (1984); G. Gerisch *et al.*, *Cold Spring Harbor Symp. Quant. Biol.* **50**, 813 (1985).
21. K. B. Raper, *J. Elisha Mitchell Sci. Soc.* **56**, 241 (1940); J. G. Williams *et al.*, *Cell* **59**, 1157 (1989).
22. J. T. Bonner, *Am. Nat.* **86**, 79 (1952); *Proc. Natl. Acad. Sci. U.S.A.* **45**, 379 (1959); J. Sternfeld and C. N. David, *Differentiation* **20**, 10 (1981); *Dev. Biol.* **93**, 111 (1982); C. J. Weijer, C. N. David, J. Sternfeld, *Methods Cell Biol.* **28**, 449 (1987).
23. B. Wang and A. Kuspa, data not shown.
24. J. Franke, G. J. Podgorski, R. H. Kessin, *Dev. Biol.* **124**, 504 (1987); L. Wu, D. Hansen, J. Franke, R. H. Kessin, G. J. Podgorski, *ibid.* **171**, 149 (1995).
25. To determine the extent of sporulation, we transferred sori from individual fruiting bodies to 20 μl of 20 mM potassium phosphate buffer (pH 6.2) containing 0.4% NP-40 nonionic detergent (Sigma) and triturated at room temperature. The number of refractile, ovoid spores was determined by phase-contrast microscopy using a hemocytometer. Spores were counted for five fruiting bodies produced by wild-type or *acaA*(PKA-C) cells.
26. The viability of the spores was determined after detergent treatment (*25*) by plating 1500 visible spores on 10 SM agar plates in association with *Klebsiella aerogenes* (*27*). The number of colonies formed was assumed to be representative of the number of viable spores in the original sample.
27. M. Sussman, *Methods Cell Biol.* **28**, 9 (1987).
28. P. Devreotes, D. Fontana, P. Klein, J. Sherring, A. Theibert, *ibid.*, p. 299.
29. The cell density dependence of development was measured by developing cells on phosphate-buffered agar at different cell densities (*27*). Cells were washed from growth media, resuspended in phosphate buffer, and diluted to various cell densities, and 0.1 ml of the suspension was spotted onto phosphate-buffered 1% agar plates (Difco, Detroit, MI). A layer of cells within a 1.8-cm^2 circle was formed after the buffer was absorbed by the agar. Total numbers of aggregates and fruiting bodies formed were scored on a dissecting microscope after 14 hours and 36 hours of development, respectively. At the highest cell density tested, some of the aggregates formed by *acaA*(PKA-C) cells, which did not progress to normal fruiting bodies, formed terminal structures similar to those observed for wild-type cells overexpressing *pkaC* (*7, 8*) or *pkaR*-null mutants (*6*). The *acaA* mutant cells were never observed to produce aggregates at these cell densities (*23*). A similar cell density dependence for aggregation of the *acaA*(PKA-C) cells was found on Millipore filters (*23*).
30. M. L. Lacombe, G. J. Podgorski, J. Franke, R. H. Kessin, *J. Biol. Chem.* **261**, 16811 (1986).
31. K. L. Fosnaugh and W. F. Loomis, *Nucleic Acids Res.* **17**, 9489 (1989).
32. S. J. McRobbie, K. A. Jermyn, K. Duffy, K. Blight, J. G. Williams, *Development* **104**, 275 (1988).
33. D. L. Richardson, C. B. Hong, W. F. Loomis, *Dev. Biol.* **144**, 269 (1991).
34. We thank W. F. Loomis, D. Hereld, and S. Lu for many helpful discussions regarding this work; G. Souza, G. Shaulsky, and W. F. Loomis for suggestions that improved the manuscript; and R. Sucgang for help in preparing the figures. Supported by grants from NIH and the State of Texas. A.K. is a Searle Scholar and an American Cancer Society Junior Faculty Research Fellow.

25 March 1997; accepted 30 May 1997

Specification of the Zebrafish Nervous System by Nonaxial Signals

Katherine Woo* and Scott E. Fraser

The organizer of the amphibian gastrula provides the neurectoderm with both neuralizing and posteriorizing (transforming) signals. In zebrafish, transplantations show that a spatially distinct transformer signal emanates from tissues other than the organizer. Cells of the germring (nonaxial mesendoderm) posteriorized forebrain progenitors when grafted nearby, resulting in an ectopic hindbrain-like structure; in contrast, cells of the organizer (axial mesendoderm) caused no posterior transformation. Local application of basic fibroblast growth factor, a candidate transformer in *Xenopus*, caused malformation but not hindbrain transformation in the forebrain. Thus, the zebrafish gastrula may integrate spatially distinct signals from the organizer and the germring to pattern the neural axis.

The developing vertebrate central nervous system is patterned by inductive interactions (*1*). The gastrula organizer (referred to as the "dorsal lip" in amphibians, "node" in amniotes, and "shield" in fish) is thought to be the source of patterning information (*2*). Analyses using amphibian embryos have indicated temporally distinct signals within the organizer (*3, 4*): An activator signal from the anterior axial mesoderm defines the anterior neurectoderm, and a subsequent transformer signal from the chordamesoderm (notochord) repatterns nearby neural tissue into more posterior types. In mouse, chick, and fish embryos, the elimination of the organizer does not abolish anteroposterior (AP) patterning in the neurectoderm; hence, there is a source of pattern information in non-organizer tissues (*5, 6*).

The neural fate map of zebrafish (*7*) shows patterning by 6 hours of development, when gastrulation has only advanced to the formation of a thickened blastoderm margin (germring) and an embryonic shield at its dorsal side. Forebrain progenitors are located far from the germring, spanning the dorsal midline (Fig. 1A). In contrast, hindbrain progenitors lie close to the germring, lateral to the embryonic shield, with midbrain progenitors in between (Fig. 1A). The early regionalization of anterior (forebrain) and posterior (hindbrain) neural progenitors within the neurectoderm allowed us to investigate signals that may differentially pattern the neuraxis. We hypothesized that proximity to the germring might specify more posterior neural fates. Indeed, labeled presumptive forebrain progenitors (Fig. 1B), transplanted (*8*) at shield stage to the position of the presumptive hindbrain, adopt the hindbrain fate (Fig. 1C). Moreover, presumptive hindbrain cells are not committed to a specific fate at this stage (*9*). Thus, the signals that normally instruct or permit cells to adopt the hindbrain fate are still active in vivo at 6 hours.

Because deletion of the shield disrupts notochord but not hindbrain development (*6*), the signals responsible for hindbrain patterning probably do not come exclusively from the shield. Germring tissue may be a source of such a posteriorizing signal. The shield contributes to axial mesoderm, notochord, and ventral neural tissues (*10*) (Fig. 1D); the germring gives rise to somitic mesoderm, posterior mesoderm, and endoderm (Fig. 1, E and F) (*11*). To investigate patterning by nonaxial germring tissue, we transplanted sectors of the shield (0°) and the germring at defined angular distances from the dorsal midline (45°, 90°, 135°, and 180°) to the animal pole, a region fated to become forebrain (Fig. 1, A and B), of shield-stage zebrafish. If the germring were the source of a patterning signal, such grafts

Division of Biology and Biological Imaging Center, Beckman Institute, California Institute of Technology, Pasadena, CA 91125, USA.

*Present address: UCSF/Gallo Center, Building 1, Room 101, San Francisco General Hospital, San Francisco, CA 94110, USA. E-mail: kwoo@itsa.ucsf.edu

should cause presumptive forebrain cells to adopt more posterior fates.

Embryos that received a fluorescently labeled germring graft to the animal pole developed hindbrain-like structures in the forebrain (Fig. 1, G to I). Ectopic host-derived structures included otic vesicles (Fig. 1H), a midbrain-hindbrain isthmus, and part of the anterior hindbrain (Fig. 1I). Large pigment cells were found near the graft site (Fig. 1H, arrows). These germring signals have a short-range effect; the contralateral forebrain appeared unaffected in recipients (Fig. 1H; see also Fig. 2C). Transplantations of ectodermal tissue into the animal pole did not cause a hindbrain transformation (*12*). At present, it is unclear which cell population (somitic mesoderm, endoderm, or both) is responsible for these transformations, because the germring contains a mixed progenitor population.

Expression analysis of Krox20, a zinc-finger transcription factor present in hindbrain rhombomeres 3 and 5 (*13*) (Fig. 2A), demonstrated that the region close to the germring transplant had adopted a hindbrain-like fate (Fig. 2, B to F, and Table 1). Ectopic Krox20 expression was detected as early as 10 to 11 hours of development (the beginning of somitogenesis), when Krox20 normally appears in the host's hindbrain (Fig. 2D); this finding suggested that the regional fate of the forebrain had been altered by the end of gastrulation (10 hours). Ectopic expression appeared as a single patch (Fig. 2, C, D, and F) or as two bands (Fig. 2, B and F). There was no obvious correlation between the origin of the graft and the amount of ectopic Krox20 induced. Ectopic otic vesicles were often found adjacent to the ectopic Krox20 expression, mimicking the normal juxtaposition of otic vesicle and rhombomere 5. Grafted tissue did not contribute to either the ectopic Krox20-expressing cells (Fig. 2C) or the ectopic otic vesicles.

In contrast, grafting the embryonic shield to the animal pole did not lead to hindbrain-like transformation (Fig. 1J and Table 1). Morphological changes in the forebrain were less drastic than those resulting from other germring grafts; the host's retina was often of near normal size (*14*) (Fig. 1J). Most of the disruption appeared to result from mechanical obstruction of forebrain morphogenesis, and perhaps from a slight expansion of the forebrain (Fig. 1J, arrowhead). Most embryos with a shield graft did not express any Krox20 in the forebrain (Fig. 2E); a minority had a few Krox20-positive cells near the graft (Table 1) (*12*).

The germring transplant's ability to change forebrain neural tissue into a section of patterned hindbrain is reminiscent of the "transforming" signal postulated to play a major role in neural patterning in *Xenopus*. Recent studies in *Xenopus* (*15*) have identified basic fibroblast growth factor (bFGF) (*4*, *16*), retinoic acid (RA) (*17*), and Wnts (*18*, *19*) as candidate transformer signals. Although there is evidence suggesting that RA acts as a posteriorizing signal in *Xenopus* (*17*), bath (*20*) or local (*21*) application of RA does not lead to a transformation of forebrain into hindbrain in zebrafish. Interfering with a number of Wnt molecules and their signaling components can result in substantial caudal defects (*22*), and there is some evidence that Xwnt3a can synergize with known neural inducers to produce a complete range of AP markers (*18*). However, no zebrafish Wnt examined to date is expressed in a pattern consistent with a transformer signal (*23*, *24*). The application of bFGF to neuralized animal caps suppresses anterior and enhances posterior neural markers (*16*), an effect expected of a transformer signal. Furthermore, overexpression of a dominant negative FGF receptor in

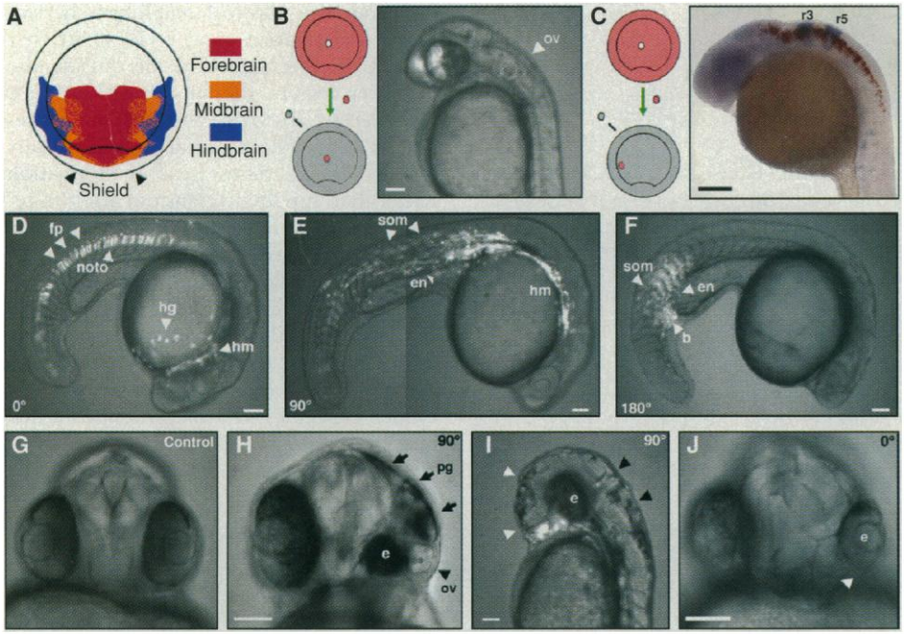

Fig. 1. Transplantation assays identifying signals important for hindbrain specification. (**A**) Neural fate map of the shield-stage gastrula, created by injecting cells with fluorescent dextran as a lineage tracer [modified from (*7*)]. (**B** and **C**) Proximity to germring tissue may be necessary for hindbrain fate. In (B), the normal fate (determined by homotopic replacement) of cells (white) located at the animal pole is to become telencephalon and retina (ov, otic vesicle). When these cells are transplanted close to the germring (C), they (brown) participate normally in the formation of the hindbrain and express Krox20 (blue) along with other host cells (r3 and r5, rhombomeres 3 and 5). (**D** to **F**) Normal descendants of the germring. Fluorescently labeled cells appear white. In (D), a homotopic graft of the central third of the embryonic shield yields labeled cells in the hatching gland (hg), head mesenchyme (hm), notochord (noto), and floorplate (fp), as previously reported (*10*). In (E), a 90° germring contains mainly somitic progenitors (som), with a minor contribution to endoderm (en) and head mesenchyme. In (F), a 180° germring contains progenitors of posterior trunk and tail somites (som), blood precursors (b), and endoderm. (**G** to **J**) Morphological changes in embryos that received mesendoderm grafts to the animal pole. A control embryo (G) is shown in frontal view. In (H), a typical embryo with a 90° germring graft has a left eye (e) that is displaced inward and downward by the ectopic hindbrain-like mass and otic vesicle. Ectopic pigment cells (pg) are present. In a case in which no ectopic otic vesicle developed (I), the graft (white) rests at the center of the anterior neuraxis, and the normal telencephalon is replaced by a tissue mass (bracketed by white arrowheads) resembling the anterior hindbrain, with the characteristic L-shaped bend of the isthmus and large pigment cells (black arrowheads). In an embryo that received a 0° (shield) graft (J), no ectopic otic vesicle or hindbrain-like mass of tissue was seen near the graft. The ventral forebrain (arrowhead) appears to be enlarged. All scale bars, 100 μm.

Table 1. Morphological and molecular changes in embryos receiving germring or shield grafts.

Type of tissue grafted	Ectopic otic vesicle(s)*		Ectopic Krox20†	
	x/m	%	*y/n*	%
45° germring	–	–	10/11	92
90° germring	18/25	72	23/23	100
135° germring	–	–	15/15	100
180° germring	23/34	68	18/18	100
0° (shield)	0/11	0	5/16	31‡

*Scored at 24 to 36 hours. †Scored at 16 to 24 hours. ‡Only a few Krox20-positive cells were detected.

zebrafish at the early cleavage stages causes a loss of posterior structures (*25*). These studies suggest that bFGF is a candidate transformer signal in zebrafish.

To determine whether local application of bFGF can mimic the transforming effect of germring tissue transplants, we implanted bFGF beads in the animal pole of shield-stage gastrula (*26*). The beads caused severe perturbation of the host's forebrain (Fig. 3B) but did not cause hindbrain-like transformation (compare Figs. 1H and 3B) or ectopic Krox20 expression (Fig. 3C). Interestingly, the expression of fore-midbrain marker *zf-otx2* (*27*) remained robust (*12*), which suggested that the regional identity of the forebrain was unchanged. Control beads not coated with bFGF had no effect on brain morphology (Fig. 3A) or gene expression (*12*). Thus, bFGF, if involved, must act in concert with other factors to generate the germring activity.

The nonaxial location of transforming activity in the zebrafish suggests a modified two-signal model (Fig. 3D): A general "activating" influence supplied by the organizer (shield) (*6*) neuralizes the presumptive neurectoderm to produce anterior neural tissue, while a transforming influence abundant in the remainder of the germring (nonaxial mesendoderm) emanates radially to posteriorize the activated (neuralized) tissue. The normal morphogenetic movements during gastrulation (*7*) displace presumptive forebrain progenitors toward the animal pole (Fig. 3D, white arrow), away from the transforming signal or signals. Hindbrain progenitors, in contrast, remain close to the germring as they converge to the dorsal side (Fig. 3D, black arrows), permitting their transformation to more posterior neural fates. Although this model differs from the classical amphibian activation-transformation model (*3*, *4*) in that the transformer signals reside outside the organizer region, the model is consistent with recent in vitro observations in zebrafish (*28*). The observation that focally applied bFGF causes head malformation rather than hindbrain transformation in zebrafish gastrula is consistent with the conclusions of a recent transgenic study using *Xenopus* (*29*), which indicated that FGFs may not be solely responsible for the neural transforming activity in vivo, in contrast to in vitro results (*16*). Our study underscores the importance of testing candidate transformer molecules in a relevant spatial and temporal context. In providing evidence for endogenous transformer action in vivo, the transformer signals might be either instructive (acting specifically to promote certain fates) or permissive. The model does not preclude the presence of other signals, for example, those that divide forebrain into telencephalon and diencephalon.

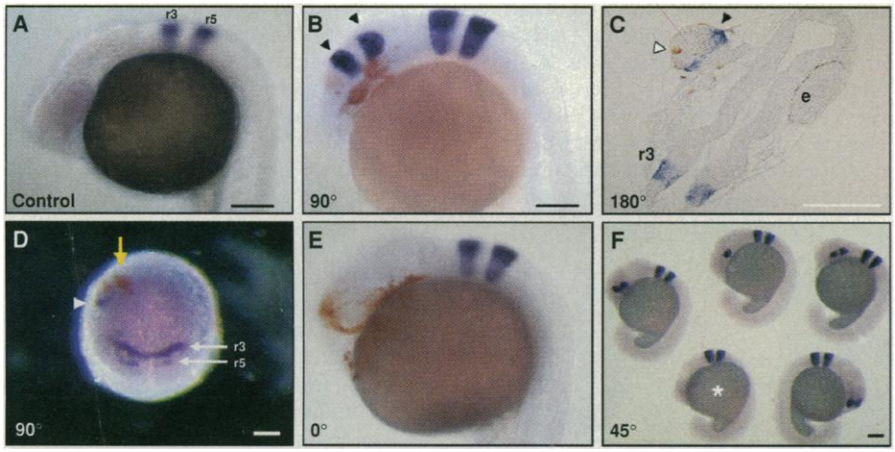

Fig. 2. Molecular changes in the forebrain after germring transplant. (**A**) Control embryo in which Krox20 (purple) marks rhombomeres 3 and 5 (r3 and r5) in the hindbrain. (**B**) In the forebrain of an embryo with a 90° germring graft (orange-brown), ectopic Krox20 expression (blue, arrowheads) indicates a transformation to hindbrain. (**C**) A section of an embryo with a 180° germring graft (e, eye). The graft (white arrowhead) does not overlap with the Krox20-positive domain (black arrowhead). (**D**) Ectopic Krox20 expression (white arrowhead) can be detected as early as 10 to 11 hours of development, when the host's normal Krox20 expression begins (white arrows). Grafted tissue (yellow arrow) did not express Krox20. (**E**) Most of the embryos with a shield graft (orange) do not have ectopic Krox20 in the forebrain. In those few that do (not shown), only a few cells are Krox20-positive. (**F**) Embryos that had received 45° germring grafts, as well as those with 135° and 180° grafts (not shown), show robust ectopic Krox20 expression near the graft in the forebrain. In a population of manipulated embryos, Krox20-positive cells are seen as one band or two bands. An asterisk marks the control embryo. All scale bars, 100 μm.

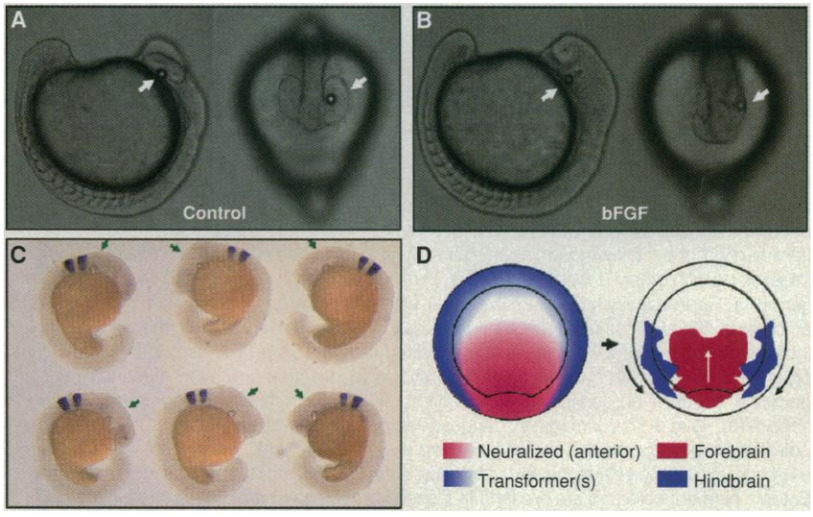

Fig. 3. Direct test of bFGF as a transformer. (**A** and **B**) Morphological changes (left panels, side view; right panels, head-on view) in the forebrain of embryos that received either control or bFGF-coated beads (arrows). Control beads (A) led to no discernible effect on forebrain morphology, whereas bFGF beads (B) caused severe forebrain deformation. In this example, the size of both optic lobes was reduced (right panels), but no hindbrain-like structure or ectopic otic vesicles were observed. (**C**) Molecular changes in embryos with bFGF beads. Unlike germring grafts (Fig. 2), bFGF does not cause ectopic expression of Krox20 in the forebrain, despite its effect on forebrain morphology (B). Green arrows point to the bead in each embryo. (**D**) Two physically separated signals acting in the zebrafish gastrula may lead to the observed neuronal fate map. An activator signal originates from the dorsal midline, perhaps before shield formation; this signal acts to induce neural tissue with a broad anterior character (red-graded area). As the germring forms, a transformer signal (blue-graded area) is generated that modulates the axial character of the nearby neural tissue, resulting in distinct forebrain (red), midbrain (not shown), and hindbrain (blue) territories. This transformer signal is strongly present within the germring and is much reduced in the shield. Dorsal ectoderm already exposed to the activator signal can react to the transformer to form the complete nervous system. The activator and trans-

model and manipulations presented here can be applied to the dissection of patterning mechanisms in the zebrafish nervous system.

REFERENCES AND NOTES

1. J. M. W. Slack and D. Tannahill, *Development* **114**, 285 (1992); D. S. Kessler and D. A. Melton, *Science* **266**, 596 (1994); O. G. Kelly and D. A. Melton, *Trends Genet.* **11**, 273 (1995).
2. H. Spemann, *Embryonic Development and Induction* (Yale Univ. Press, New Haven, CT, 1938); T. Doniach, *J. Neurobiol.* **24**, 1256 (1993); A. Ruiz-i-Altaba, *ibid.*, p. 1276.
3. P. D. Nieuwkoop *et al.*, *J. Exp. Zool.* **120**, 1 (1952); H. Eyal-Giladi, *Arch. Biol.* **65**, 179 (1954); M. Sala, *Proc. K. Ned. Akad. Wet. Ser. C* **58**, 635 (1955); L. Saxen and S. Toivonen, *Primary Embryonic Induction* (Logos, London, 1962).
4. T. Doniach, *Cell* **83**, 1067 (1995); I. Mason, *Curr. Biol.* **6**, 672 (1996).
5. S.-L. Ang and J. Rossant, *Cell* **78**, 561 (1994); D. C. Weinstein *et al.*, *ibid.*, p. 575; D. Psychoyos and C. Stern, *Development* **122**, 3263 (1996).
6. J. Shih and S. E. Fraser, *Development* **122**, 1313 (1996).
7. K. Woo and S. E. Fraser, *ibid.* **121**, 2595 (1995).
8. Donor embryos were injected, at the two- to four-cell stage, with a 1:1 mixture of rhodamine and biotin dextrans (50 mg/ml, Molecular Probes), which allowed for subsequent detection of grafted cells both fluorescently and histochemically. All surgical manipulations were performed by established methods with the use of an eyelash-hair knife and hairloop in full-strength Danieau solution (*6*). Embryos were then raised individually in 24-well plates. Microscopic documentation was performed as described (*7*). Full-color documentation was performed with a ProgRes 3012 digital color camera and ImageManager software (Roche Image Analysis Systems).
9. K. Woo and S. E. Fraser, *Dev. Biol.* **170**, 764 (1995); in preparation.
10. J. Shih and S. E. Fraser, *Development* **121**, 2755 (1995).
11. At shield stage, nonaxial germring cells share molecular characteristics distinct from the shield region: They express *snail1* [M. Hammerschmidt and C. Nüsslein-Volhard, *ibid.* **119**, 1107 (1993); C. Thisse, B. Thisse, T. F. Schilling, J. H. Postlethwait, *ibid.*, p. 1203] and *eve1* (S. Joly, C. Joly, S. Schulte-Merker, H. Boulekbache, H. Condamine, *ibid.*, p. 1261), and they down-regulate *zf-T* as gastrulation proceeds [S. Schulte-Merker, R. K. Ho, B. G. Herrmann, C. Nüsslein-Volhard, *ibid.* **116**, 1021 (1992)].
12. K. Woo and S. E. Fraser, data not shown.
13. In situ hybridization of Krox20 was performed as described [E. Oxtoby and T. Jowett, *Nucleic Acids Res.* **21**, 1087 (1993)]. Grafted cells were visualized by incubating post–in situ embryos overnight with streptavidin–horseradish peroxidase (Molecular Probes), then developing with diaminobenzidine, yielding an orange-brown color.
14. In 30% of the cases, presumably because the graft had occupied most of the retinal domain on its side, a morphologically normal retina on the side of the graft was not formed. In section, however, pigmented epithelium and some retinal tissues were present.
15. Reviewed in H. Sive and L. Bradley, *Dev. Dyn.* **205**, 265 (1996); Y. Sasai and E. M. DeRobertis, *Dev. Biol.* **182**, 5 (1997).
16. W. G. Cox and A. Hemmati-Brivanlou, *Development* **121**, 4349 (1995); M. Kengaku and H. Okamoto, *ibid.*, p. 3121; T. M. Lamb and R. M. Harland, *ibid.*, p. 3627.
17. A. J. Durston *et al.*, *Nature* **340**, 140 (1989); N. Papalopulu *et al.*, *Development* **113**, 1145 (1991); C. R. Sharpe, *Neuron* **7**, 239 (1991); B. Blumberg *et al.*, *Development* **124**, 373 (1997).
18. L. L. McGrew, C.-J. Lai, R. T. Moon, *Dev. Biol.* **172**, 337 (1995).
19. R. T. Moon, J. D. Brown, M. Torres, *Trends Genet.* **13**, 157 (1997).
20. N. Holder and J. Hill, *Development* **113**, 1159 (1991).
21. G. A. Hyatt *et al.*, *ibid.* **122**, 195 (1996).
22. S. Takada *et al.*, *Genes Dev.* **8**, 174 (1994); Y. Yoshikawa, T. Fujimori, A. P. McMahon, S. Takada, *Dev. Biol.* **183**, 234 (1997); I. Dominguez, K. Itoh, S. Y. Sokol, *Proc. Natl. Acad. Sci. U.S.A.* **92**, 8498 (1995). Interfering with some Wnt members and their signaling cascade causes axis duplication (*18, 23*) [X. He *et al.*, *Science* **275**, 1652 (1997)].
23. G. M. Kelly, P. Greenstein, D. F. Erezyilmaz, R. T. Moon, *Development* **121**, 1787 (1995).
24. S. Krauss, V. Korzh, A. Fjose, T. Johansen, *ibid.* **116**, 249 (1992); G. M. Kelly, C.-J. Lai, R. T. Moon, *Dev. Biol.* **158**, 113 (1993); G. M. Kelly and R. T. Moon, *Dev. Genet.* **17**, 129 (1995); P. Blader, U. Strähle, P. W. Ingham, *Dev. Genes Evol.* **206**, 3 (1996).
25. K. Griffin, R. Patient, N. Holder, *Development* **121**, 2983 (1995).
26. The bFGF bead-coating procedure was adopted from Z. Dai and H. B. Peng [*J. Neurosci.* **15**, 5466 (1995)]. Polystyrene beads (Polysciences, 45 μm) were coated with a solution of bFGF (50 μg/ml; human recombinant, Gibco) for 2 hours at room temperature, then washed twice (10 min each) with large volumes of Danieau solution (*6*). One or two beads were implanted into the animal pole region of shield-stage embryos. In most animals, the beads remained in the forebrain; in a few cases, the beads drifted posteriorly or into the yolk, and these were excluded from further analysis. The functional activity of the beads was tested with a modified animal cap assay, in which five to eight beads were sandwiched between two pieces of stage 8.5 animal caps and cultured in modified Barth solution until stage 10.5. Sandwiches with bFGF beads underwent morphogenetic movements similar to those treated with soluble bFGF. Sandwiches made with beads not coated with bFGF developed in the same way as control caps without beads.
27. Y. Li, M. L. Allende, R. Finkelstein, E. Weinberg, *Mech. Dev.* **48**, 229 (1994).
28. C. G. Sagerström, Y. Grinblat, H. Sive, *Development* **122**, 1873 (1996).
29. K. L. Kroll and E. Amaya, *ibid.*, p. 3173.

30. We thank T. Jowett and E. Weinberg for probes, J. Shih for advice on transplantation, M. Selleck and C. LaBonne for advice on bead experiments, and A. Collazo, C. Krull, C. LaBonne, A. Louie, E. Krider, J. Shih, P. Sternberg, B. Wold, K. Zinn, and two anonymous reviewers for comments. Supported by grants from the Beckman Institute and by a National Institute of Mental Health Silvio Conte Center award.

8 October 1996; accepted 27 May 1997